BENCHMARKING IMPEDANCE CALCULATIONS FOR TWO TYPES OF TRANSITION STRUCTURES IN HALF: CST VS. ECHO3D

Xin Huang[1], Haiyan Yao[1], Jincheng Xiao[1], Tianlong He*[1]
[1]National Synchrotron Radiation Laboratory, USTC, Hefei 230029, China

Abstract

Photon masks and tapered transitions in the Hefei Advanced Light Facility (HALF) storage ring are typical transition structures that can make non-negligible contributions to the geometric impedance. In this work, ECHO3D is used to benchmark the CST calculations for these two types of structures. The longitudinal and transverse wake potentials, the corresponding impedance spectra, and the resulting loss factor, kick factor, and effective impedance are analyzed and compared. This study provides a reference for impedance evaluation of these transition structures in HALF.

INTRODUCTION

The Hefei Advanced Light Facility (HALF) is a diffraction-limited storage-ring light source currently under construction [1]. In the storage ring, 11 tapered transitions will be installed in Phase-I to match the small-gap insertion-device chambers to the vacuum pipe with a diameter of 26 mm. In addition, 248 photon masks are installed in the ring to intercept synchrotron radiation and protect sensitive vacuum components. Previous studies have shown that both tapered transitions and photon masks can make non-negligible contributions to the impedance budget of HALF: tapered transitions because of their relatively large single-element impedance, and photon masks because of their large number [2].

Previous results for these two types of structures were obtained using CST Wakefield Solver [3]. To assess their reliability, ECHO3D [4] is used in this work to benchmark the CST calculations. The models of the photon mask and tapered transition are shown in Fig. 1. For benchmarking purposes, the central elliptical pipe section in the tapered-transition model is shortened to 30 mm to reduce the computational cost. In the actual HALF design, this section has two lengths, 1.95 m and 4.56 m. The main parameters of the photon masks and tapered transitions are summarized in Tables 1 and 2, respectively.

To resolve the geometric impedance up to 200 GHz and the short-range wakefield details, a Gaussian bunch with an rms length of 0.5 mm is used in both codes. In CST, the wakefield solver with the indirect-interfaces integration method is employed to handle the concave geometries. The longitudinal and transverse mesh sizes in CST are approximately 25 μm and 50 μm, respectively. In ECHO3D, the corresponding mesh sizes are 50 μm and 100 μm, respectively, following Ref. [5]. Test calculations show that the ECHO3D results are essentially converged with respect to the longitudinal mesh, whereas further refinement of the transverse mesh is limited by the available computer memory. The resulting wake potentials and impedance spectra are then used to evaluate the loss factor, effective impedance, and kick factor for the benchmark.

* htlong@ustc.edu.cn

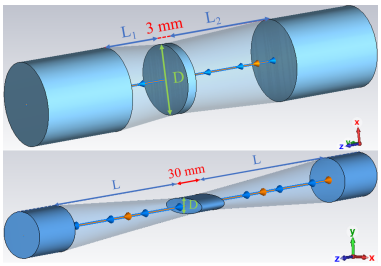

Figure 1: Schematic models of the photon mask (top) and the tapered transition (bottom).

Table 1: Summary of photon-mask parameters. Types 1, 2, and 3 correspond to (L_1, L_2) values of $(37, 20)$, $(32, 20)$, and $(25, 15)$ mm, respectively. The listed β functions are averages over all corresponding locations.

Component	D [mm]	Type	β_x [m]	β_y [m]	N_{elem}
Mask 1	22.8	1	5.90	9.04	20
Mask 2	24	1	4.11	6.65	20
Mask 3	23.2	1	2.18	3.71	20
Mask 4	20	2	1.41	5.88	20
Mask 5	22	1	2.97	2.54	20
Mask 6	24	3	2.33	3.78	20
Mask 7	20.4	1	2.59	7.69	20
Mask 8	24	1	7.94	6.96	16
Mask 9	24	1	7.94	6.96	4
Mask 10	24	1	6.24	8.64	2
Mask 11	24	1	6.24	8.64	6
Mask 12	20	1	1.51	14.67	20
Mask 13	20.4	1	3.37	11.71	20
Mask 14	22	2	5.79	7.73	20
Mask 15	20.8	1	7.78	5.22	20

Table 2: Summary of tapered-transition parameters. The average beta functions at the tapered-transition locations are $\beta_x = 6.99$ m and $\beta_y = 3.12$ m.

Component	D [mm]	L [mm]	N_{elem}
Wiggler	8	110	2
HU115	9	110	1
EPU120	12.6	110	1
EPU42/46/63	8	110	3
EPU44A/44B	8	50	2
LPU38A/38B	8	110	2

BENCHMARK QUANTITIES

The total longitudinal and β-weighted transverse impedances for each component family are obtained by direct summation:

$$Z_{\parallel}^{\mathrm{tot}}(\omega) = \sum_{j}^{\text{elements}} Z_{\parallel,j}(\omega), \tag{1}$$

$$\beta Z_{\perp}^{\mathrm{tot}}(\omega) = \sum_{j}^{\text{elements}} \beta_{\perp,j} Z_{\perp,j}(\omega). \tag{2}$$

Based on the impedance spectrum, the loss factor, effective impedance, and kick factor as functions of the rms bunch length σ_z are calculated as:

$$k_{\parallel}(\sigma_z) = \frac{1}{\pi}\int_0^{\infty} \mathrm{Re}\left[Z_{\parallel}^{\mathrm{tot}}(\omega)\right] |\lambda(\omega)|^2 d\omega, \tag{3}$$

$$\mathrm{Im}Z_{\parallel}/n = \frac{\displaystyle\int_{-\infty}^{\infty} \mathrm{Im}[Z_{\parallel}^{\mathrm{tot}}(\omega)]\frac{\omega_0}{\omega}|\lambda(\omega)|^2 d\omega}{\displaystyle\int_{-\infty}^{\infty}|\lambda(\omega)|^2 d\omega}, \tag{4}$$

$$\beta k_{\perp}(\sigma_z) = \frac{1}{\pi}\int_0^{\infty} \mathrm{Im}\left[\beta Z_{\perp}^{\mathrm{tot}}(\omega)\right] |\lambda(\omega)|^2 d\omega, \tag{5}$$

where $\lambda(\omega) = e^{-\omega^2\sigma_z^2/2c^2}$ is the frequency domain distribution of a Gaussian bunch, and ω_0 is the angular revolution frequency. Here, $k_{\parallel}$ represents the energy loss per unit charge, $\mathrm{Im}Z_{\parallel}/n$ characterizes the influence of low-frequency longitudinal impedance on potential well distortion, and $k_{\perp}$ characterizes the average transverse deflecting effect of the transverse impedance on the bunch. These expressions are applied to the CST and ECHO3D simulation results for the benchmark.

BENCHMARK RESULTS FOR PHOTON MASKS

Figure 2 compares the total longitudinal and β-weighted vertical wake potentials and impedances of the photon masks. The two codes agree well in the long-range wakefield region, but differ visibly in the short-range region ($s \leq 2$ mm). Similar short-range differences were also reported in Ref. [6]. The largest differences appear in the vertical impedance and in the high-frequency longitudinal impedance. In the vertical direction, the imaginary impedance from ECHO3D has an almost constant offset of about 20.3 kΩ, about 45% of the trapped-mode impedance peak from CST. In the longitudinal direction, the imaginary impedance from ECHO3D differs from that from CST by about 67% at 50 GHz. By contrast, the horizontal wake potential and impedance agree well.

Figure 3 shows the loss factor and effective impedance derived from the longitudinal impedance, while Fig. 4 shows the kick factors derived from the transverse impedance. The loss factor and horizontal kick factor agree well with the CST results, whereas the effective impedance from ECHO3D differs from CST by about 17%, due to the difference in the imaginary longitudinal impedance, and the vertical kick factor differs by about 64%.

Overall, for the photon masks, good agreement is observed for the horizontal plane and low-frequency longitudinal impedance. However, significant discrepancies exist in the vertical imaginary impedance and high-frequency longitudinal imaginary impedance, which directly impact the derived integrated parameters. The transverse discrepancies may be related to the limited transverse mesh resolution in the ECHO3D simulations; the underlying cause is still under investigation.

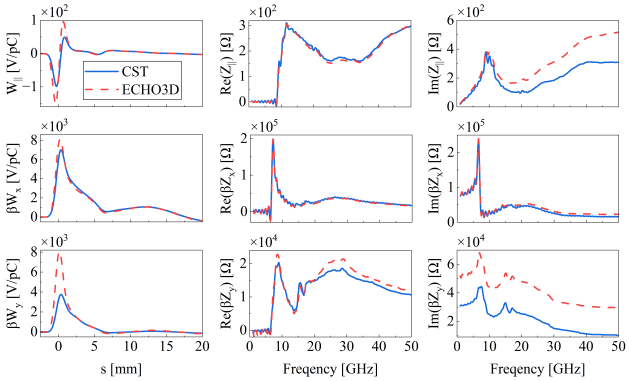

Figure 2: Comparison of the total longitudinal wake potential and impedance, and the β-weighted total transverse wake potential and impedance, for the photon masks.

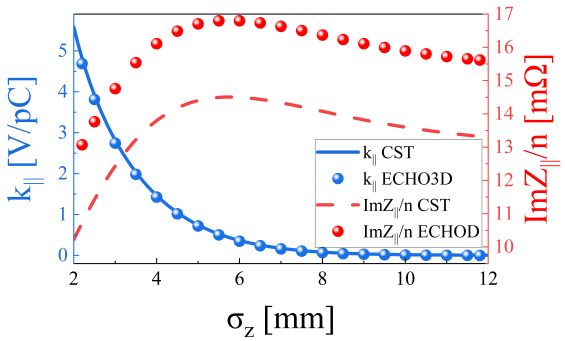

Figure 3: Loss factor and effective impedance of the photon masks versus rms bunch length.

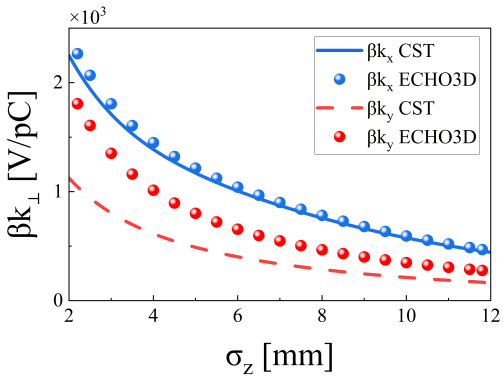

Figure 4: β-weighted kick factor of the photon masks versus rms bunch length.

BENCHMARK RESULTS FOR TAPERED TRANSITIONS

For the tapered transitions, the corresponding wake potentials and impedances are shown in Fig. 5. The two codes agree well in the long-range wakefield region, and the short-range differences are much smaller than those for the photon masks. In the horizontal direction, the imaginary impedance shows an almost constant offset of about 4.43 kΩ, about 9% of the maximum impedance below 50 GHz. In the longitudinal direction, good agreement is obtained at low frequencies, while visible differences appear only above 50 GHz.

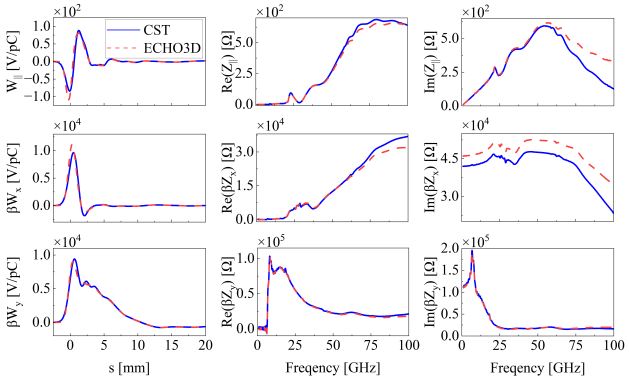

Figure 5: Comparison of the total longitudinal wake potential and impedance, and the β-weighted total transverse wake potential and impedance, for the tapered transitions.

Figure 6 shows that the loss factor also agrees well between the two codes, while the effective impedance differs by only about 2%. This is consistent with the better agreement of the tapered-transition impedance over a wider frequency range. Figure 7 shows that the kick factors also agree well between the two codes.

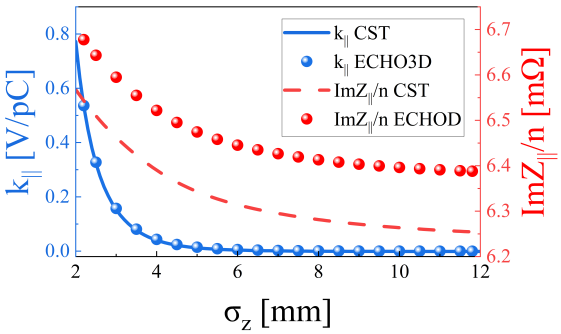

Figure 6: Loss factor and effective impedance of the tapered transitions versus rms bunch length.

For the tapered transitions, the benchmark shows very good overall agreement across all quantities, providing strong confidence in the reliability of the CST results for this class of structures.

CONCLUSION

The CST results for photon masks and tapered transitions in HALF are benchmarked against ECHO3D by comparing the wake potentials, impedance spectra, and the corresponding loss factor, effective impedance, and kick factor. Very good agreement is obtained for the tapered transitions, indicating that the CST results are reliable for this type of structure. For the photon masks, the two codes agree well in the horizontal direction and at low longitudinal frequencies, but show clear differences in the vertical impedance and in the high-frequency longitudinal impedance. As a result, noticeable differences also appear in the effective impedance and vertical kick factor. Therefore, the CST results for photon masks should be treated with caution in the vertical direction and at high frequencies. The reason for these differences is still under investigation, but they may be related to the transverse mesh in ECHO3D.

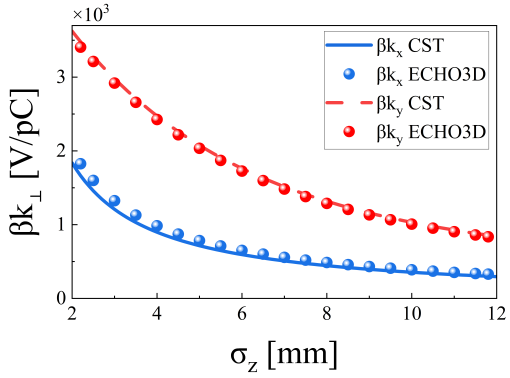

Figure 7: β-weighted kick factor of the tapered transitions versus rms bunch length.

ACKNOWLEDGEMENT

This work was supported by the National Natural Science Foundation of China (Nos. 12375324 and 12105284) and the Fundamental Research Funds for the Central Universities (No. WK2310000127).

REFERENCES

[1] Z. Bai *et al.*, "Progress on the Storage Ring Physics Design of Hefei Advanced Light Facility (HALF)," in *Proc. IPAC'23*, Venice, Italy, May 2023, pp. 1075–1078. doi:10.18429/JACoW-IPAC2023-MOPM038

[2] T. He *et al.*, "Beam coupling impedance modeling for the Hefei Advanced Light Facility", presented at the *Proc. IPAC'26*, Normandy, France, May 2026, paper THP5645, this conference.

[3] Dassault Systèmes, *CST Studio Suite*. https://www.3ds.com/products/simulia/cst-studio-suite

[4] I. Zagorodnov, *ECHO3D*. https://echo4d.de

[5] A. Khan and V. Smaluk, "Convergence Study of Wakefield Simulations with GdfidL and ECHO3D," *Nucl. Instrum. Methods Phys. Res. A*, vol. 1082, p. 171073, 2026. doi:10.1016/j.nima.2025.171073

[6] G. Wang *et al.*, "Impedance Calculation for the Hadron Storage Ring in the Electron-Ion Collider with ECHO3D," in *Proc. IPAC'24*, Nashville, TN, USA, May 2024, pp. 3104–3107. doi:10.18429/JACoW-IPAC2024-THPC48